Progress in Organic Coatings 172 (2022) 107071

Contents lists available at ScienceDirect

Progress in Organic Coatings

journal homepage: www.elsevier.com/locate/porgcoat

# Exploring the protection mechanism of a combined fluoropolymer coating on sulphide patinated bronze

Tadeja Kosec [a,*], Živa Novak [a], Erika Švara Fabjan [a], Luka Škrlep [a], Matjaž Finšgar [b]

[a] Slovenian National Building and Civil Engineering Institute, Dimičeva ulica 12, SI-1000 Ljubljana, Slovenia
[b] Faculty of chemistry and chemical engineering, University of Maribor, Smetanova ulica 17, SI-2000 Maribor, Slovenia

ARTICLE INFO

*Keywords:*
Bronze
Sulphide patina
Corrosion
Protection
Electrochemistry
FIB-SEM
XPS

ABSTRACT

When bronze or artificially patinated bronze is exposed to an outdoor environment that contains aggressive ions such as sulphates, nitrates, and carbonates, the surface of the bronze changes its appearance due to the formation of corrosion products on the surface. Research is being conducted on versatile protective measures that can be used to protect the surface from these changes. A recently synthesised fluoropolymer-based coating with mercaptopropyl groups, i.e. a 3-component fluoropolymer coating FA-MS-SH (silane-modified poly methylmethacrylate (MS) with added mercaptopropyltrimethoxy silane (SH) and a fluoroacrylate (FA)) was explored in detail in this work where its protective mechanism on sulphide patinated bronze was investigated. Electrochemical tests were conducted on the sulphide patinated bronze with and without the 3-component coating FA-MS-SH. Furthermore, FA, MS and SH alone and various combinations and concentrations of FA-MS were studied in order to determine the protective effect and properties of each component. Colour change and contact angle measurements were also defined. FIB-SEM measurements and GCIB-XPS depth profiles were carried out to study surface bonding with the sulphide patina in detail.

A mechanism for the protection of sulphide patinated bronze was presented through the use of a multi-analytical tool approach. It was shown that FA physisorbed on the patinated surface, while MS and blends of the components chemisorbed on the layer of sulphide patinated bronze, also resulting in the surface being efficiently protected from corrosion processes.

## 1. Introduction

Bronze surfaces, whether bare or patinated, are prone to change when exposed to a humid aggressive environment, especially in polluted urban atmospheres [1]. In order to prevent discolouration and retain the artistic texture and appearance of bronze statues the protection of bronze from corrosion is very important in the conservation of bronze surfaces. Ideally protection should be clear, removable, and mitigate corrosion [2].

Finding efficient coating for corroded or artificially patinated surfaces is of special interest and challenge at the same time. Up to two decades ago, coatings have been developed and studied especially on bare bronze surfaces, with majority of the research focused on inhibitor interaction with bronze surfaces [3–5]. However, bare bronze behaves very differently from patinated surfaces, when unprotected or protected, having different affinity to form chemisorbed layer of benzotriazole-BTA inhibitor on freshly prepared bronze surfaces and constituent metals and silicon [5,6]. First reports on protecting patinated surfaces date back to 2007 when electrochemical patina was formed simulating archaeological patina and different inhibitors were tested, among which tolylmethylimidazole was most efficient, but less than BTA [7]. More studies on effectiveness of inhibition efficiency were done on chemical, electrochemical, ancient and historical patinas [8,9]. Later on, different protections were studied on patinated bronzes including brown, chloride and nitrate patina. It was found that different protection systems, including inhibitors, waxes, Paraloid B44, protected patinated surfaces to a different extent [10–13] while the effectiveness of inhibitors was especially related to the chemistry of artificially patinated surface [14]. It was shown that methylbenzimidazole efficiently protected chloride patina but not sulphide patina, where BTA was more efficient. In order to efficiently protect patinated surfaces, it is of huge importance to master the properties of naturally formed patinas [15,16] and artificially formed patinas that also represent unique surface and unique properties [17–19]. As such sulphide patina is of special interest since it is widely

* Corresponding author.
*E-mail address:* tadeja.kosec@zag.si (T. Kosec).

https://doi.org/10.1016/j.porgcoat.2022.107071
Received 28 April 2022; Received in revised form 26 July 2022; Accepted 28 July 2022
Available online 5 August 2022

**Table 1**
Presentation of the samples tested by different techniques.

| Sample | Sample/ coating[a] | Electrochemical tests, contact angle and colour measurements | XPS, AFM | FIB-SEM |
|---|---|---|---|---|
| Unprotected patina | | Yes | | |
| Single component coating | MS (x = 1, 5, 10, 20) | Yes | Yes (MS10) | |
| | FA5 | Yes | Yes (FA5) | |
| | SH10 | Yes | | |
| Double component coating | MS10-SHx (x = 1, 5, 10) | Yes | | |
| | FAx-MS10 (x = 1, 5, 10) | Yes | Yes (FA5-MS10) | |
| Triple component coating | FA1-MS10-SH5 (single layer) | Yes | | |
| | FA1-MS10-SH5 (2 layers) | | | |
| | FA5-MS10-SH5 (single layer) | Yes | Yes (FA5-MS10-SH5-single layer) | Yes |
| | FA5-MS10-SH5 (2 layers) | Yes | | |

[a] The number beside the description of the coating refers to the wt% in the overall mixture.

adopted way of treating bronze surfaces used by conservators and restorers nowadays.

Fluoropolymer coatings with their unique properties have been proposed for versatile applications.

Fluorine based superhydrophobic coatings have been developed by functionalization of silica nanoparticles with fluorinated groups for the use on aluminum, glass and silicon substrates with reported excellent properties [20]. Due to their excellent mechanical properties, chemical resistance, and non-stick properties, fluoropolymer coatings are used to replace chromium electroplating on brass [20,21]. One study showed that incorporating fluoroalkyl chains in silica-based coatings resulted in crack-free layers, a smooth surface, high transparency, and increased hydrophobicity, showing great potential for flexible photonic structures [22]. Lately, protection from long-term corrosion has been demonstrated using siloxane polyacrylic sol-gel coatings containing alkyl and perfluoroalkyl chains developed for aluminum alloys [23].

The use of a fluoropolymer coating on bronze is also being explored [6,24,25]. Such an idea has already been pioneered by Bierwagen et al., who tried to find longer lasting, durable, and corrosion resistant protection systems for bronze in order to replace waxes and acrylic-based coatings (introduced commercially as product Incralac®) [6]. They reported that a polyvinylidene fluoride coating showed excellent barrier properties on bronze, but the adhesion was poor [6]. Covalent modification of Laponite clay with fluoroalkyl silanes was reported to occur via a reaction between the hydroxyl groups on the edge of the clay sheet and a silane bond to produce covalent siloxane bonds [24]. Such composite films on bronze showed many improved properties, such as reduced water sensitivity, polymer degradation by UV light and increased barrier properties [24]. It was also reported that polyhedral oligomeric silsesquioxane-POSS nanoparticles addition enhanced hydrophobicity and protective efficiency of fluoropolymer coating on bare bronze while mechanical properties decreased [25].

In B-IMPACT project, the newly developed fluoropolymer coating FA-MS was shown to offer efficient and long term protection for aged bronze surface simulating natural exposure of bronze to outdoor environment [26]. In the following study from the same group of authors,

**Table 2**
Contact angles values and colour variations in the various samples following the application of different coatings, samples further explored by XPS are marked with *.

| Sample | Sample/ coating* | Contact angle/° | $\Delta L$ | $\Delta a$ | $\Delta b$ | $\Delta E^*$ |
|---|---|---|---|---|---|---|
| Unprotected patina | Sulphide patina | 92 ± 5 | / | / | / | / |
| Single component coating | MS1 | 78 ± 1 | −10.3 ± 0.3 | 1.9 ± 0.2 | 3.1 ± 0.3 | 11 ± 0 |
| | MS5 | 76 ± 0 | −16.3 ± 0.5 | 2.3 ± 0.2 | 3.7 ± 0.4 | 17 ± 0 |
| | MS10* | 78 ± 1 | −17.8 ± 0.8 | 2.4 ± 0.9 | 1.3 ± 0.4 | 18 ± 1 |
| | MS20 | 75 ± 4 | −15.8 ± 0.6 | 1.5 ± 0.1 | 1.5 ± 0.4 | 16 ± 0 |
| | FA5* | 114 ± 2 | −11.7 ± 0.7 | 4.8 ± 0.6 | 3.7 ± 0.2 | 13 ± 1 |
| | SH10 | 67 ± 10 | −14.5 ± 0.2 | 3 ± 1 | −1.1 ± 0.3 | 15 ± 0 |
| Double component coating | MS10-SH1 | 69 ± 2 | −14 ± 1 | 4.1 ± 0.5 | 4.8 ± 0.3 | 15 ± 1 |
| | MS10-SH5 | 65 ± 2 | −14.9 ± 0.9 | 5.9 ± 0.7 | 10.5 ± 0.8 | 19 ± 1 |
| | MS10-SH10 | 62 ± 3 | −20.2 ± 0.5 | 1.6 ± 0.3 | 3.9 ± 0.3 | 21 ± 1 |
| | FA1-MS10 | 115.8 ± 0.6 | −12 ± 1 | 0.5 ± 1.1 | −2 ± 1 | 13 ± 1 |
| | FA5-MS10* | 115.9 ± 0.8 | −11 ± 2 | 2.5 ± 0.6 | 0.2 ± 0.6 | 11 ± 2 |
| | FA10-MS10 | 114 ± 2 | −13 ± 1 | −1 ± 0 | 0.8 ± 0.2 | 13 ± 1 |
| Triple component coating | FA1-MS10-SH5 (single) | 115.8 ± 0.7 | −18 ± 2 | 3 ± 1 | 4 ± 1 | 19 ± 3 |
| | FA1-MS10-SH5 (2L) | 113 ± 1 | −15 ± 2 | 3.6 ± 0.5 | 5.6 ± 0.5 | 17 ± 3 |
| | FA5-MS10-SH5* (single) | 116.4 ± 0.5 | −21 ± 2 | 2 ± 2 | −1.2 ± 0.6 | 21 ± 2 |
| | FA5-MS10-SH5 (2L) | 112 ± 2 | −15 ± 2 | 0.8 ± 0.4 | 0.8 ± 0.7 | 15 ± 2 |

the FA-MS coating and FA-MS-SH coating were studied on sulphide and sulphate patinated surfaces in order to find efficient protection for such surfaces [27]. 3-Mercapto-propyl-trimethoxysilane (Prop-SH) was selected as the additive to a fluoropolymer coating due to studies reported previously. Namely, propS-SH was proved to be very effective for corrosion mitigation in copper [28], bronzes and gilded bronzes [13] and patinated bronzes exposed to simulated natural environment [29]. In the following studies it was shown to give excellent protection also to a sulphide patinated surfaces [19].

Using fluoropolymer coating FA-MS-SH [27], model of mechanism of protection was then suggested but not verified with appropriate experimental methods. In the present study, the different single, dual and triple components of that coating are blended, electrochemically tested and a few of them spectroscopically investigated on sulphide patinated bronze in order to define effects of single, double, triple components of the fluoropolymer coating and their relation to protective efficiency.

The focus of this work is to investigate the corrosion mechanism of a fluoropolymer coating on sulphide patinated bronze. Firstly,

**Table 3**
Electrochemical parameters $E_{corr}$ (red from Figs. 2 and 3) and mean values of $R_p$, as deduced from multiple linear polarization measurements and calculated protection efficiency η, according to Eq. (1).

| Sample | Sample/coating | $E_{corr}$/ mV | $R_p$/kΩ $cm^2$ | η % |
|---|---|---|---|---|
| Unprotected patina | Sulphide patina | −72.2 | 4 | – |
| Single component coating | MS1 | −48.7 | 21 | 81.3 ± 1.9 |
| | MS5 | −16.0 | 1300 | 99.2 ± 0.9 |
| | MS10 | −54.9 | 4090 | 99.9 ± 0.1 |
| | MS20 | −43.5 | 8100 | 99.7 ± 0.4 |
| | FA5 | 7.52 | 20 | 79.8 ± 4.7 |
| | SH10 | −32.6 | 5 | 24.3 ± 16 |
| Double component coating | MS10-SH1 | −176 | 6950 | 99.9 ± 0.1 |
| | MS10-SH5 | −11.5 | 3700 | 99.9 ± 0.0 |
| | MS10-SH10 | −64.9 | 13,100 | 99.8 ± 0.2 |
| | FA1-MS10 | −106 | 2040 | 97.5 ± 3.2 |
| | FA5-MS10 | 4.05 | 920 | 84.4 ± 13 |
| | FA10-MS10 | −114 | 3200 | 92.7 ± 9.9 |
| Triple component coating | FA1-MS10-SH5 (single) | −114 | 7100 | 99.9 ± 0.1 |
| | FA1-MS10-SH5 (2L) | −91.7 | 7900 | 99.3 ± 1.1 |
| | FA5-MS10-SH5 (single) | −35.2 | 9580 | 99.4 ± 0.9 |
| | FA5-MS10-SH5 (2L) | −6.24 | 9300 | 99.2 ± 0.7 |

electrochemical methods were used to evaluate the corrosion protection of the 3-component fluoropolymer coating (FA-MS-SH) on sulphide patinated bronze, as well as the performance of each of the components individually and various combinations thereof (FA, MS, SH). Colour and hydrophobicity (contact angle) measurements were also performed. Secondly, detailed surface analyses of the coated patinated bronze were performed using focused ion beam scanning electron microscopy (FIB-SEM) and X-ray photoelectron spectroscopy (XPS) depth profiling in association with gas cluster ion beam (GCIB) sputtering.

## 2. Material and methods

### 2.1. Preparation of samples and application of the coatings

#### 2.1.1. Bronze and patination

The chemical composition of a quaternary as-cast sample of bronze (CuSn6Zn4Pb2), determined after digestion by optical emission spectroscopy, was 88.10 wt% Cu, 5.28 wt% Sn, 3.84 wt% Zn and 2.71 Pb wt %. Bronze samples were cut into discs of 15 mm diameter. All samples were then ground with 1200-grit SiC paper and ultrasonically cleaned in ethanol for 3 min.

The bronze samples were then patinated with a brown patina by 3-ply brushing a heated (80 °C) bronze surface with 3 % $K_2S$ solution. The surface was then rinsed with distilled water in order to remove any poorly adhered flakes of $Cu_2S$ from the surface. All chemicals were of p. a. quality.

#### 2.1.2. Preparation of the coatings

Fluoropolymer (FA) was obtained by drying a commercial solution of polyfluoroacrylate (Funcosil AG by Remmers, Crawley, UK).

Methacryloxypropyl-trimethoxysilane (MS) was synthesised by copolymerizing methyl methacrylate and methacryloxypropyl-trimethoxysilane at a 9:1 molar ratio for 72 h at 55 °C, using acetone as a solvent and 2 % lauroyl peroxide as an initiator. Synthesis of (MS) as the adhesion promoter has been described in detail previously [26]. After polymerization, diethyl succinate was added and the acetone was evaporated to form a 20 vol% solution. This solution was used as basis to formulate different coatings.

3-Mercapto-propyl-trimethoxysilane (SH) as a coating and diethylsuccinate and *n*-butylacetate as solvents were obtained from Sigma Aldrich.

For a layer-by-layer application, FA was dissolved in *n*-heptane to form 1, 5 and 10 wt% solution. All other coatings were formulated in a solvent mixture of diethylsuccinate and *n*-butylacetate in a 3:2 mass ratio. For a layer-by-layer application the second layer (FA in *n*-heptane) was applied after the first layer had dried and further cured at 40 °C for 2 h.

All coatings were applied as described previously [26] using a coverage of 4.4 ± 2 mg per 15 mm diameter sample (around 25 g/$m^2$).

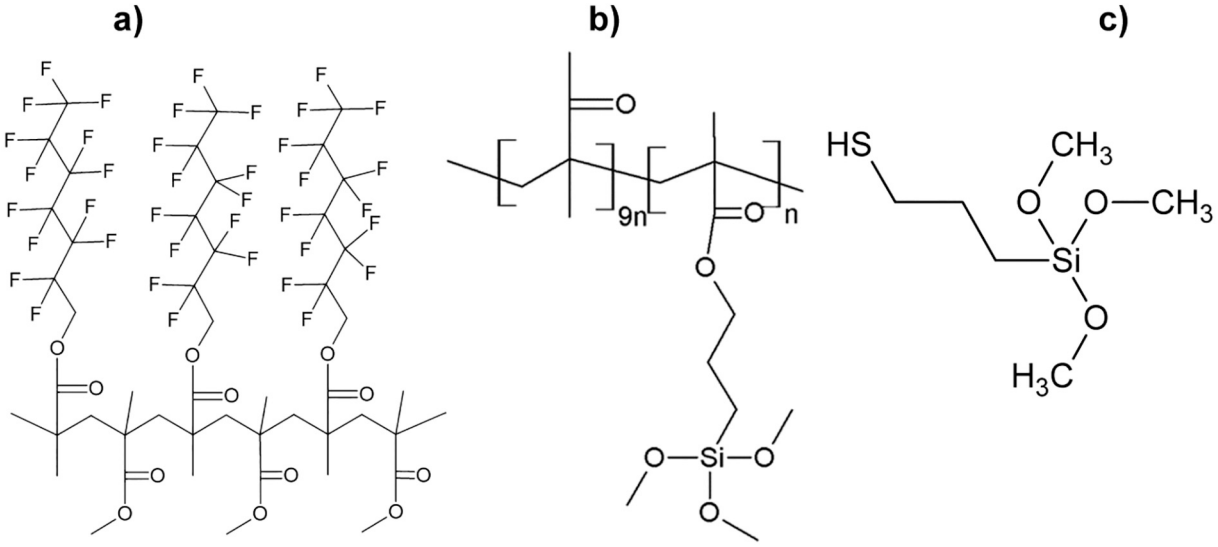


**Fig. 1.** Components of the fluoropolymer coating: fluoroacrylate-FA (a), methacryloxypropyl-trimethoxysilane-MS (b), and 3-mercapto-propyl-trimethoxysilane-SH (c).

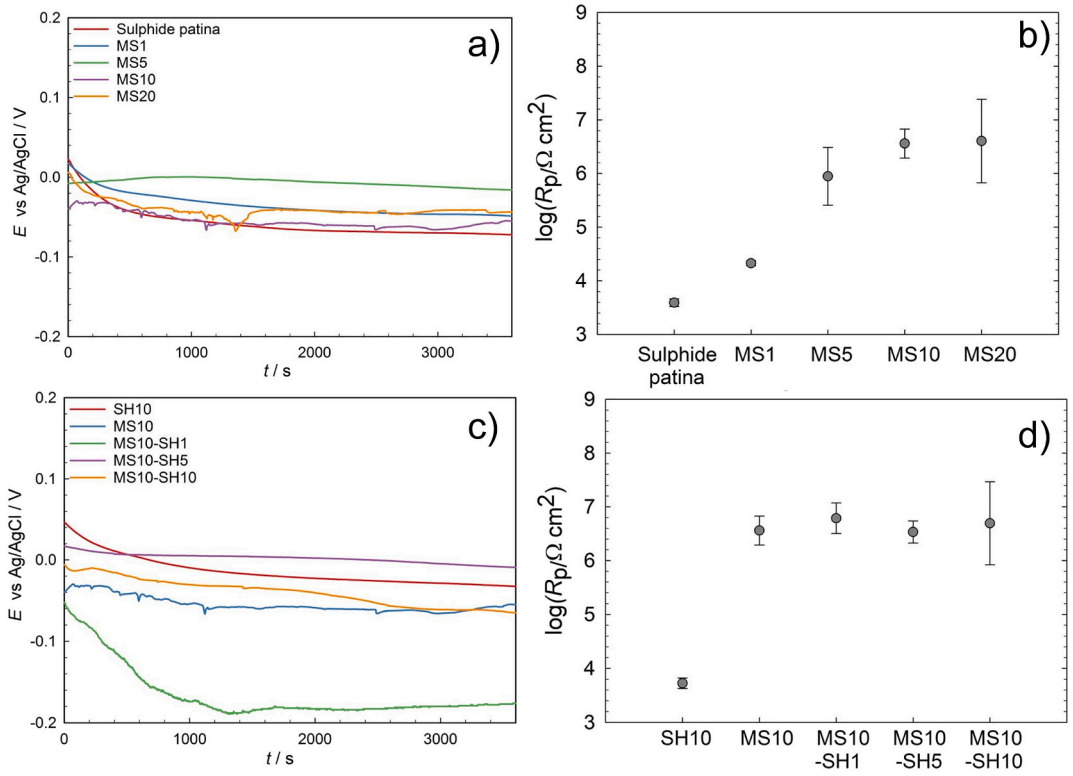


**Fig. 2.** Open circuit potential and log $R_p$ diagram with standard deviation of log $R_p$ values for sulphide patinated bronze both with and without the different types of protective coating (MSx (x = 1, 5, 10, 20) and MS10-SHx (x = 1, 5, 10)).

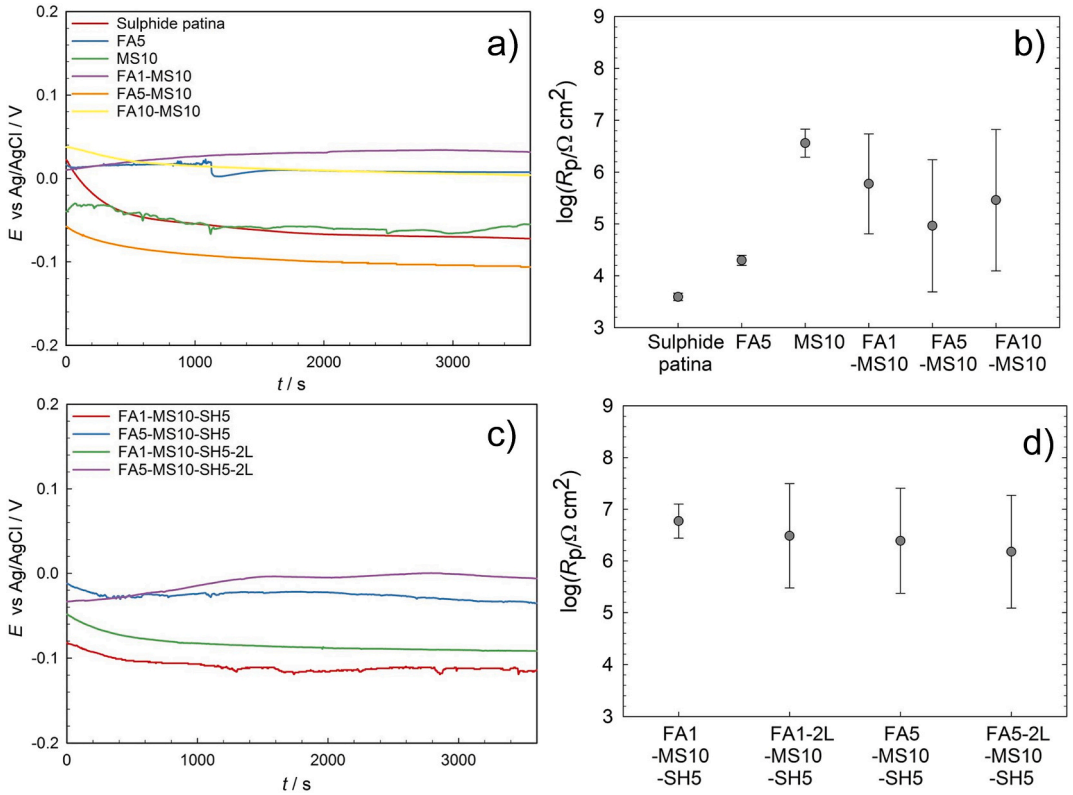


**Fig. 3.** Open circuit potential and log $R_p$ diagram with standard deviation of log $R_p$ values for the sulphide patinated bronze both with and without the different types of protective coating (FA5 and MS10-FAx (x = 1, 5, 10) and FA-MS-SH).

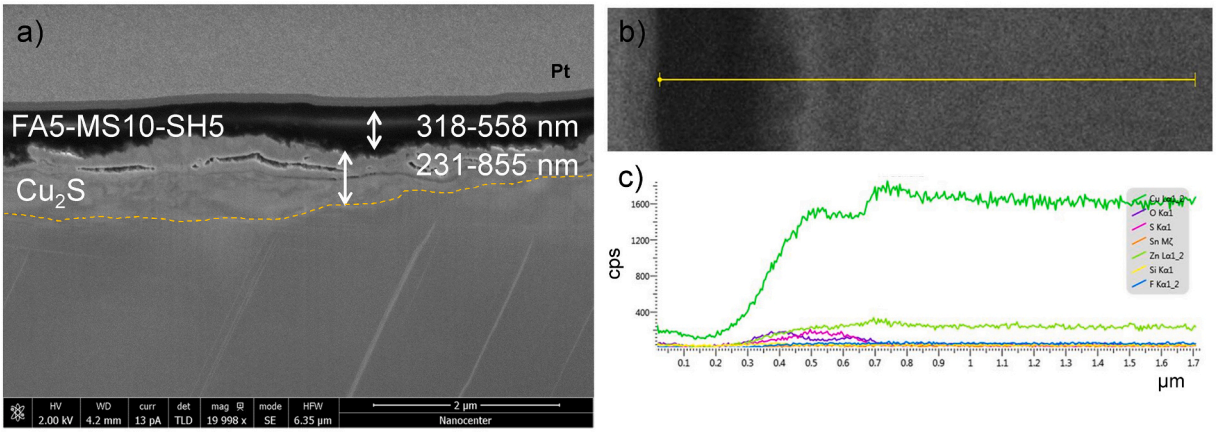


**Fig. 4.** FE-SEM image of the FIB milled cross-section of a FA5-MS10-SH5 coated sulphide patinated bronze (a), FE-SEM image b) and cps graph c) for different elements along the line showed in b.

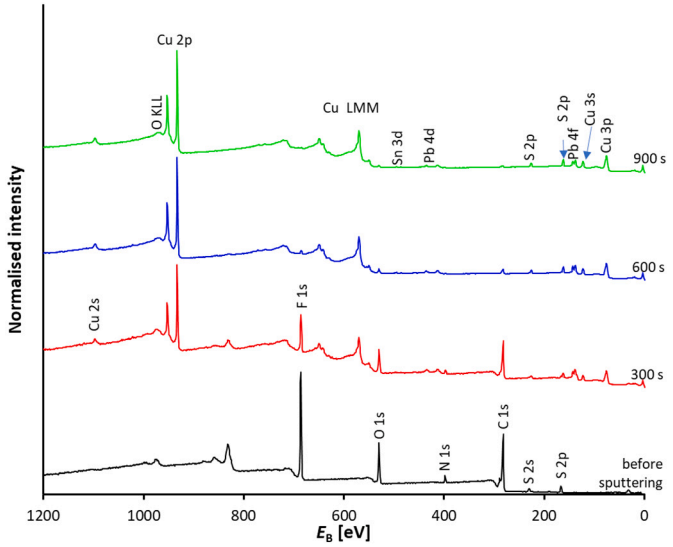


**Fig. 5.** XPS survey spectra for the FA5 sample before and after sputtering with 10 keV $Ar^{+}_{1000}$ (sputtering time is designated on the right-hand side).

The coated samples were dried for around 2 h under room conditions and cured at 40 °C and a relative humidity of 98 % for at least 20 h.

The designation of different coatings is composed of component abbreviation and wt% content. For the SH component wt% is based on dry MS content.

### 2.1.3. Application of the protective coatings and curing

The following coatings were prepared for electrochemical evaluation: MS coatings applied over the patinated surface at concentrations of 1 wt% (MS1), 5 wt% (MS5), 10 wt% (MS10), and 20 wt% (MS20), SH alone at a concentration of 1 wt% SH (indicated as SH10 - content based on the dry MS content), and MS10 combined with either 1 wt% SH (MS10-SH1), 5 wt% SH (MS10-SH5) or 10 wt% SH (MS10-SH10). The different combinations were then combined with FA: 5 % FA (FA5), FA1-MS10, FA5-MS10, FA10-MS10 and FA1-MS10-SH5, FA5-MS10-SH5. A combination of the latter two mixtures was then tested using a 2 layer application as well (FA1-MS10-SH5-2L, FA5-MS10-SH52L). Altogether, the patina and 16 different coatings were analysed, including electrochemical testing, contact angle and colour change measurements following application of the coatings (see Table 1).

### 2.2. Electrochemical testing

Electrochemical testing of the patinated bronze and various coatings was conducted in 1000-times concentrated urban rain at a pH of 5.4 with conductivity of 3.716 mS/cm at 22 °C that enables reliable electrochemical measurements. The simulated urban rain solution contained 685.7 mg $SO_4^{2-}$, 287.0 mg/L $Cl^{-}$, and 943.2 mg/L $NO_3^{-}$.

All electrochemical measurements were conducted using Gamry Frameworks on a Gamry Reference REF 600+ potentiostat/galvanostat in a three-electrode cell with an Ag/AgCl (sat. KCl) reference electrode and a graphite counter electrode. All potentials in the text refer to the Ag/AgCl (sat. KCl) electrode.

Firstly, open circuit potential was measured for at least 1 h, or until a stable potential was attained. Linear polarization measurements were then executed in the potential range ±20 mV vs $E_{corr}$ at a scan rate of 0.1 mV/s. A minimum of three measurements were conducted in replicate and the average values and standard deviations then determined.

Protection efficiency, η, was calculated using the following Eq. (1):

$$\eta\% = \left[1 - \left(R_p/R_p'\right)\right] \times 100 \quad (1)$$

where $R_p'$ is the protected and $R_p$ the unprotected polarization resistance value, as deduced from linear polarization measurements. Polarization resistance was defined as the tangent value fitted to the curve at $j = 0$.

### 2.3. Surface characterisation and spectroscopic analysis

#### 2.3.1. FIB-SEM analysis

FEG-SEM FEI Helios NanoLab 600i with an energy dispersive X-ray spectroscopy (EDS) detector (Aztec Oxford apparatus, SDD detector, WD 4 mm) was used for detailed study of the coated bronze. The sample was Pt nanocoated in the range 15 × 5 μm. The in situ cross-sections were obtained by FIB milling ($Ga^{+}$ ions). An accelerating voltage of 2 kV and current intensity of 12 pA were used for the surface and cross-section imaging.

#### 2.3.2. Colour variations

Colour variations of samples were evaluated using the method previously presented [26]. The *Lab* values (CIE 1976 $L^*a^*b^*$ or CIELAB colour space) were measured at three different areas on each sample, both before and after the coating was applied. An i1 colourimeter (X-Rite) device was used, which operates with a 45/0 measuring geometry, a D65 illuminant and a 5-mm sample aperture. The total colour difference, $\Delta E^*$, was calculated using Eq. (2). The non-coated sample was used as a reference for the calculation of $\Delta E^*$, where

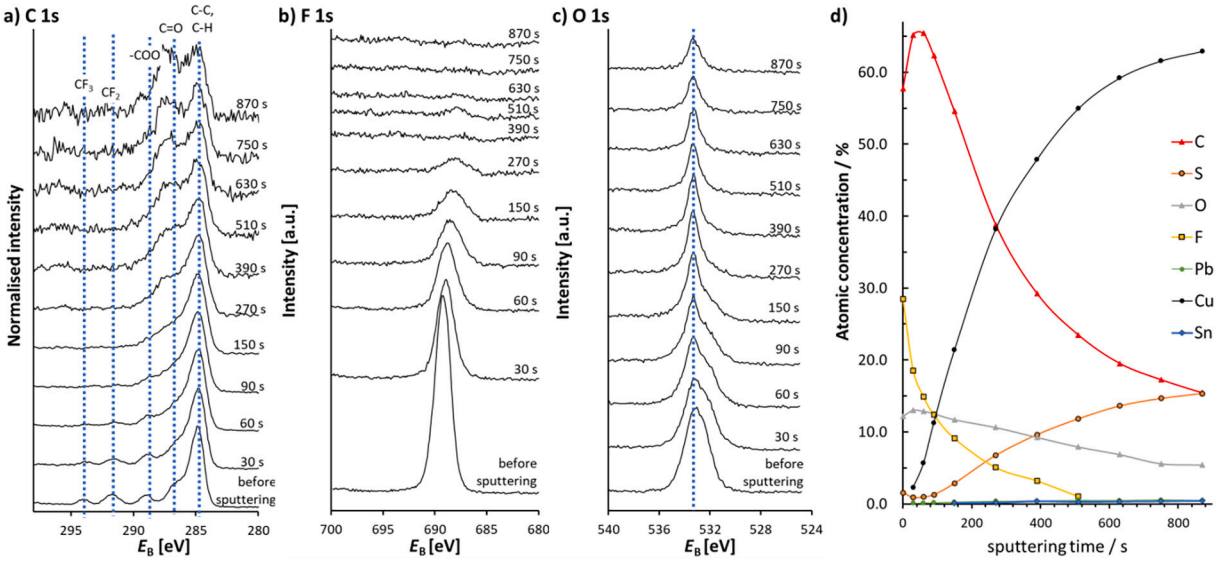


**Fig. 6.** HR a) C 1s, b) F 1s and c) O 1s spectra for the FA5 sample before and after sputtering with an $Ar^+_{1000}$ ion beam, and d) the corresponding XPS depth profile.

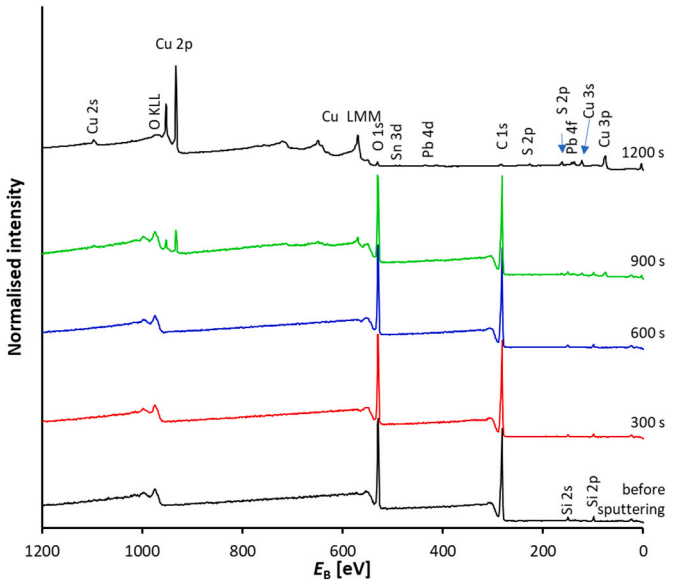


**Fig. 7.** XPS survey spectra for the MS10 sample before and after sputtering with 10 keV $Ar^+_{1000}$ (sputtering time is designated on the right-hand side).

$$\Delta E^* = \left(\Delta L^{*2} + \Delta a^{*2} + \Delta b^{*2}\right)^{1/2} \quad (2)$$

### 2.3.3. XPS and AFM measurements

XPS measurements were performed using a Supra+ instrument (Kratos, Manchester, UK) equipped with an Al $K_\alpha$ source, a monochromator, and a charge neutralizer. The take-off angle of the analysis, i.e. the angle to the surface, was 90°. The charge neutralizer was turned on during acquisition of the XPS spectra. The binding energy ($E_B$) scale was corrected using the C-C/C-H peak in the C 1s spectrum at 284.8 eV. Data were acquired and processed using ESCApe 1.4 software (Kratos, Manchester, UK). An analysis spot, 110 μm (diameter) in size, was created in the center of the sputtering crater by rastering a 2 by 2 mm sized spot with a gas cluster ion beam (GCIB) using 10 keV $Ar^+_{1000}$. The pass energy used to acquire high-resolution (HR) and survey spectra was 40 eV and 160 eV, respectively. Quantification to obtain a depth profile was performed by normalizing the surface atomic concentrations to 100.0 %. A Shirley background subtraction was used [30].

AFM measurements were performed with an MFP 3D Origin Plus instrument (Asylum/Oxford Instruments, Santa Barbara, CA, USA) in tapping mode using an OMCL-AC240TS-R3 silicon cantilever (Olympus Micro Cantilever, Taibei, Taiwan). The analysis was performed on a spot size of 20 by 20 μm.

### 2.3.4. Measurement of the contact angle

Contact angle measurements were executed using the static method with an FTA 1000 DropShape Instrument B FrameSystem (First Ten Angstroms, Newark, USA). A 2 μL droplet of distilled water was deposited on the samples (with at least three measurements made per sample) and an image documented. The Young–Laplace equation was used for fitting and determination of the contact angle. The results are presented as the average of the three values measured.

## 3. Results and discussion

### 3.1. Hydrophobicity and colour change following application of the coating

Average values of the sample surface contact angle measurements and colour variations are given in Table 2.

The contact angle for the unprotected patinas was low (92 ± 5°). The application of single component coatings of MS and SH does not increase the contact angle of the protected surface. When the FA5 coating was applied to the patinated surface, the contact angle was increased (114 ± 2°). Also, double component coatings with FA component had increased value of a contact angle, similar was observed for triple component coatings, whether applied as single layer or applied as two layers (Table 2).

Variations in the colour of the samples following the application of different coatings were evaluated by colour differences ($\Delta E^*$), as presented in Table 3. The application of different coatings on the brown patinated samples resulted in $\Delta E^*$ values between 11 and 21 (see Table 2). $\Delta E^*$ for single component coating (MS) refer to values between $\Delta E^* = 11$ (for MS1) and $\Delta E^* = 18$ (for MS10), the value for the most concentrated single layer component (MS20) is $\Delta E^* = 16$. $\Delta E^*$ for FA5 component is 13, for the SH10 $\Delta E^* = 15$. Application of double component coating (MS10-SH) with variation in concentration in SH component result in values between $\Delta E^* = 15$ and $\Delta E^* = 21$, the highest $\Delta E^*$ correspond to the most concentrated sample (MS10-SH10). Application of triple component single application coating (FA1-MS10-SH5) results in $\Delta E^* = 19$, whereas double layer application coating FA1-

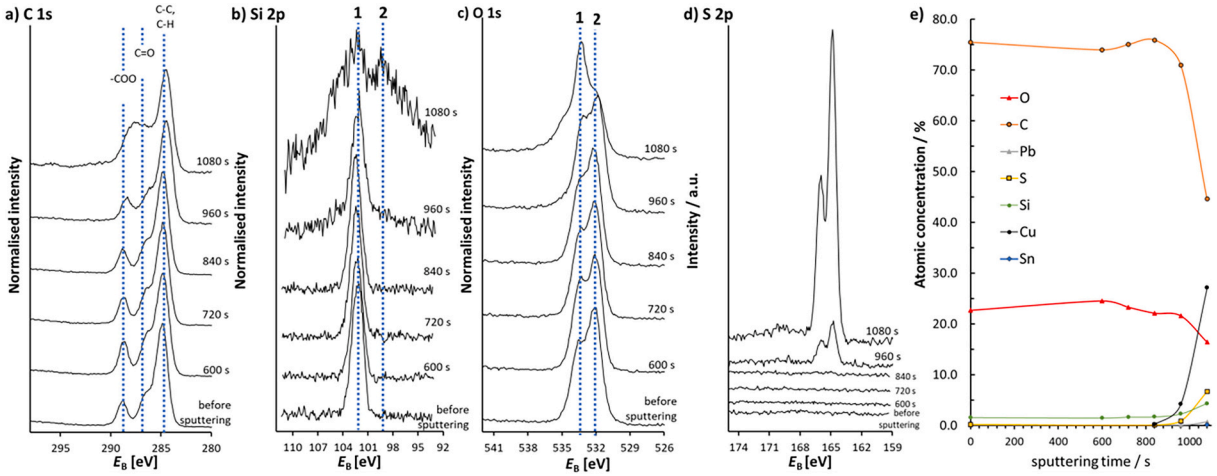


**Fig. 8.** HR a) C 1s, b) Si 2p, c) O 1s, and d) S 2p spectra for the MS10 sample before and after sputtering with an $Ar^+_{1000}$ ion beam (sputtering time is designated for each spectrum), and e) the corresponding XPS depth profile.

MS10-SH5 (2L) in the $\Delta E^* = 17$. Triple component coating with higher amount of FA (FA5-MS10-SH5, FA5-MS10-SH5, 2L) result in $\Delta E^* = 21$ and $\Delta E^* = 15$. It can be seen from Table 2 that the standard deviations for single component coatings are smaller than in the case of double component coating, and they were even higher for triple component coatings. This observation also reflects the uneven coating when applied over the brown patinated surface, especially in the case of when fluoroacrylate (FA) component is present in the coating, which has been already previously described [26].The main contribution to the colour variations in all analysed samples corresponds to a change in lightness (ΔL, see Table 2), with contributions also in $\Delta a$ and $\Delta b$ components. According to a report by Mokritzky et al., colour differences (ΔE) values between 11 and 21 correspond to a difference that would be noticeable as two different colours to the standard observer (defined for the values $\Delta E^* > 5$) [31]. It can be concluded that the application of coatings affects the change in colour in all samples to the extent that the difference in colour, i.e. mainly as the darkening of the samples, could be clearly observed by the visual observation.

### 3.2. Electrochemical evaluation of single and combined coatings on sulphide patinated bronze

The results of open circuit potential and linear polarization measurements for the patinated bronze, both with and without the different types of protective coating, are presented in Figs. 2 and 3. Corrosion potential, $E_{corr}$, and mean values of multiple measured polarization resistances, $R_p$, were extracted from the linear polarization measurements (see Table 3).

Open circuit potential is most negative in the sulphide patinated bronze (Fig. 2a), while, in general, the MS coating shifts open circuit potential to more positive values. Mean values of polarization resistance, $R_p$, is the lowest for the sulphide patinated bronze without any coating, and increases for the samples with MS coatings, with the MS1 sample having the lowest value (Fig. 2b, Table 3). Increasing the concentration of MS in the solution from 1 to 20 wt% increased the $R_p$ value from 21 kΩ cm$^2$ to 8100 kΩ cm$^2$. The application of an SH-only coating does not protect the surface from the processes of corrosion, while using combinations of MS10-SHx (x = 1, 5, and 10) resulted in very high $R_p$ values. The concentration of SH in the solution does not have an impact, as can be seen from the lack of impact on the $R_p$ values. Logarithms of the $R_p$ values, with standard deviations of the replicate measurements, are given in Fig. S1 in the Supplement.

When FA5 or FAx-MS10 (x = 1, 5, 10) coating is applied, the open circuit potential shifts to more positive values (Fig. 3a), except FA5-MS10 which shifted to more negative potentials. Only slightly increased $R_p$ value was observed for FA5 coating when compared to unprotected sulphide patina. Application of the FAx-MS10 (x = 1, 5, 10) combination increased mean value of $R_p$ to 2040, over 920 to 3200 kΩ cm$^2$ with similar values and large standard deviation. Combinations of FA-MS-SH resulted in very high mean values of $R_p$ with large standard deviations, suggesting a protection efficiency of >99.2 %, as estimated from Eq. (1) (Fig. 3d, Table 3). Linear polarization curves for the one closest to mean values given in Figs. 2 and 3 are given in Figs. S1 and S2 in the Supplement.

It is important to note that reported variation of $R_p$ values is not uncommon for patinated bronze since patina may be quite uneven. Furthermore, it shows that the system under investigation, which includes uneven patina and various coatings produces large variability of measurements where proper use of statistical methods is very important.

### 3.3. FIB-SEM analysis

The in-situ cross sections of the FA5-MS10-SH5 coating on sulphide patinated bronze at specific representative locations were observed in order to estimate the thicknesses of the patina and coating. The choice of this particular coating for FIB SEM analysis stems from our previous coatings with similar concentrations applied over brown patinated bronze [27]. The image of the cross section is presented in Fig. 4a, with the line elemental compositions obtained from EDS analysis presented in Fig. 4b.

The FA5-MS10-SH5 coating evenly covers the patinated surface. The coating is 318–558 nm thick, while the sulphide patina layer is 231–855 nm thick. The patinated layer is not uniform, and horizontal cracks are evident, confirming the presence of $Cu_2S$, which is flaked and does not fully adhere to the surface. Similar findings have been reported previously [19]. The FA5-MS10-SH5 coating covers the patinated layer and adheres well to the surface, confirming the good barrier properties shown by the electrochemical results. It can be observed from the line elemental analysis that the outer layer consists of an organic coating, in which the signals for S, O, and Cu intensify towards the center. Sulphur is present in both the coating and the copper sulphide (i.e. the patina layer), while oxygen is also present in the coating and to some extent in the patinated layer. The FIB-SEM analysis showed that the FA5-MS10-SH5 coating evenly covered the patina across the entire surface, to varying degree of thickness.

### 3.4. XPS analysis

A detailed XPS study was conducted to determine the bonding properties of the multi-component fluoropolymer coatings applied to the

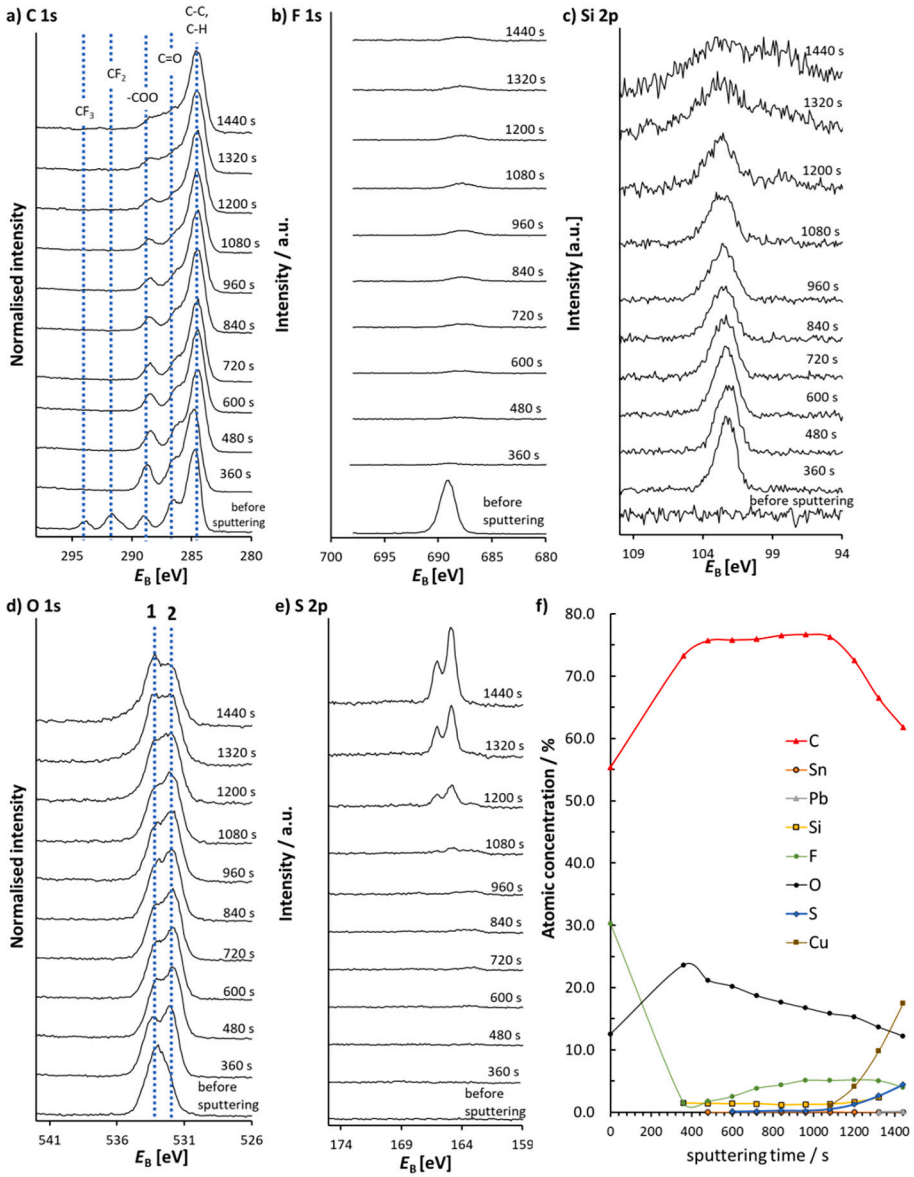


**Fig. 9.** HR a) C 1s, b) F 1s, c) Si 2p, d) O 1s, and e) S 2p spectra for the FA5-MS10 sample before and after sputtering with an $Ar^+_{1000}$ ion beam (sputtering time is designated for every spectrum), and f) the corresponding XPS depth profile.

sulphide patinated bronze. For the XPS study, the following coatings on sulphide patinated bronze were analysed: FA5, MS10, FA5-MS10 and FA5-MS10-SH5.

### 3.4.1. *FA5 coating on sulphide patinated bronze*

Fig. 5 shows survey spectra for FA5 coating on patinated bronze obtained before and after sputtering for 300, 600, and 900 s with 10 keV $Ar^+_{1000}$. Before sputtering, the surface contained signals for F, C, O and N. The signals for F, C, O are from fluoropolymer (see Fig. 1a). Oxidized adventitious carbonaceous species may also contribute to the C and O signals. After sputtering for 300 s with 10 keV $Ar^+_{1000}$, the signals show that $Cu_2S$ covers the substrate, i.e. Cu 2p, Cu LMM, Cu 3p, Cu 3s, S 2p, and S 2s, indicating that the coating has been partially removed, and also that the signal originates from the surface of the substrate ($Cu_2S$ on patina). Moreover, after 300 s of sputtering, Sn 3d and Pb 4f signals also develop, as the substrate also contains Sn and Pb. At the same time, the signal for F-containing species (F 1s), which are part of the coating, also significantly decreases.

Fig. 6 shows the HR spectra in the FA5 sample measured before and after each sputtering cycle during the depth profiling. The spectra representing the topmost position (the lowest spectra in Fig. 6a) contain peaks on the more positive $E_B$ side of the main peak, and correspond to carbon bonded to three and two flourine atoms ($CF_3$ and $CF_2$, binding energies at approx. 294 and 292 eV, respectively, as indicated by the dashed lines). These peaks significantly decrease after the first sputtering cycle and disappear after 90 s of sputtering. Moreover, the spectral features corresponding to the COO (ester) with binding energy at 289 eV, and C═O groups at 286 eV, remain intense after the second sputtering cycle (Fig. 6a). The latter means that the fluoropolymer is oriented with $CF_3$ and $CF_2$ towards the surface, and with the ester and C═O groups towards the substrate, as shown in Fig. 1a. The HR non-normalized F 1s spectra in Fig. 6b further confirm this. The lowest F 1s spectrum, representing the surface before sputtering, is the most intense, and this then drops significantly after each sputtering cycle. In addition, the lowest O 1s spectra in Fig. 6c, representing the topmost position, are broader than those representing the position closer to the surface (the highest spectra in Fig. 6c). An additional contribution to the O 1s signal, that may result in the broadening of spectra for the topmost surface, may also arise from the presence of oxidized adventitious carbonaceous species. The position of the center of the O 1s spectra,

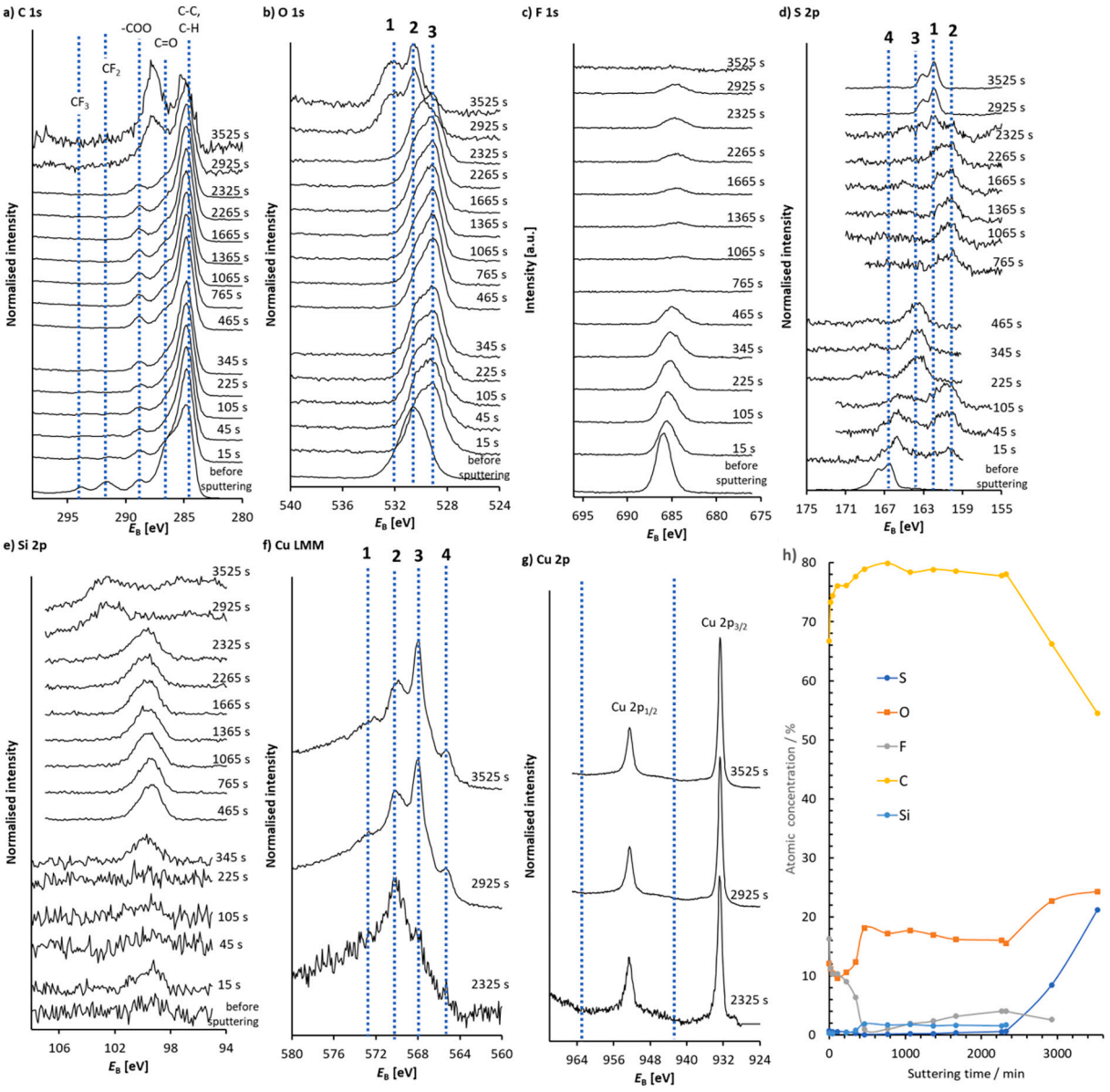


**Fig. 10.** HR a) C 1s, b) O 1s, c) F 1s, d) S 2p, e) Si 2p, f) XPS-induced Auger Cu LMM, and g) Cu 2p spectra for the FA5-MS10-SH5 sample before and after sputtering with an $Ar^{+}_{1000}$ ion beam (sputtering time is designated for each spectrum), and h) the corresponding XPS depth profile.

however, remains constant during sputtering. The latter indicates that the fluoropolymer is not chemisorbed on the substrate, which probably explains the lower protection efficiency in comparison to other coatings. The corresponding depth profile, based on the HR spectra obtained during depth profiling of the FA5 sample, is shown in Fig. 6d. Since the substrate contains Pb and Sn, and is covered with $Cu_2S$, the atomic concentration at the surface increases in line with the sputtering time.

### 3.4.2. *MS10 coating on sulphide patinated bronze*

Fig. 7 shows survey spectra for the MS10 sample. The surface consists of Si, C, and O signals (the lowest spectrum in Fig. 7 represents the measurement before sputtering). After 900 s of sputtering, the signals for Cu 2p and XPS-induced Cu LMM become intense (and signals for S 2s and S 2p also develop), indicating that the sputter beam has partially removed the coating and that the excitation signal has reached the substrate.

Fig. 8a shows the HR C 1s spectra, with spectral features representing COO, C═O, and C-C/C-H. The most significant change in the shape of the C 1s spectra occurs after 1080 s of sputtering, corresponding to changes in COO and C═O. Simultaneously, the same change occurs in the Si 2p spectra. The feature at $E_B$ 103 eV, representing silanes (an intense signal up to 960 s of sputtering, positioned at the dashed line 1 in Fig. 8d), and the feature at $E_B$ 100 eV (dashed line 2, Fig. 8d), correspond to SiC, which might be present on the substrate surface due to the use of SiC grinding papers in the preparation of samples.

Fig. 8c shows the O 1s spectra, with two spectral features marked by the dashed lines 1 ($E_B$ = 533.4 eV) and 2 ($E_B$ = 532.0 eV). We assumed that the O environment at dashed line 2 represents the O species in the MS10 coating (such as O in C═O/COO groups), while its appearance at dashed line 1 is most likely related to the O atoms (attached to Si) that connect the MS10 to the substrate. Fig. 8c shows that the most significant change in the O environment occurs between 960 s and 1080 s of sputtering, where the main peak shifts from position 2 to position 1 (Fig. 8c). The latter may indicate that MS is adsorbed on the surface via O atoms. This adsorption occurs on the $Cu_2S$, with the signal first appearing after sputtering for 960 s (Fig. 8d). The MS10 coating is also thicker than FA5, as shown by the fact that in the former the signal was obtained from the substrate after a longer sputtering time.

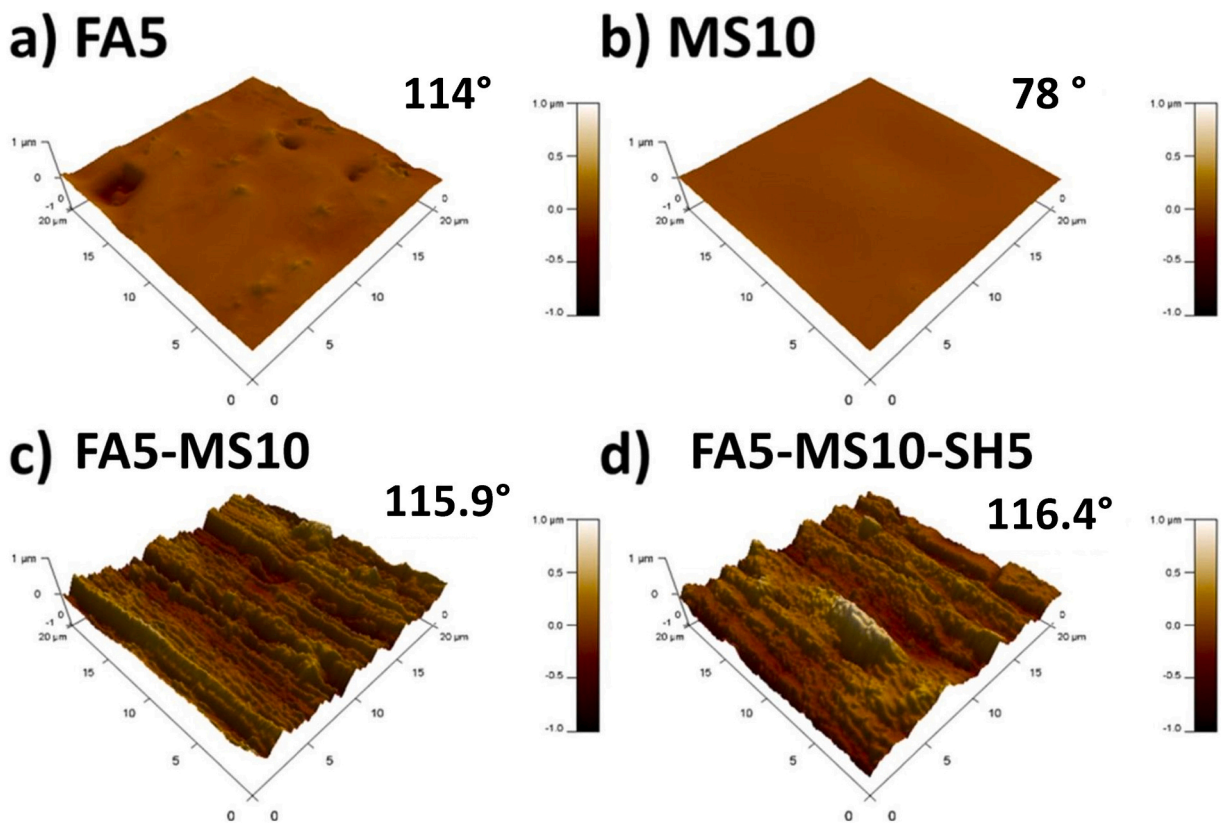


**Fig. 11.** Topography of the a) FA5, b) MS10, c) FA5-MS10, and d) FA5-MS10-SH5 samples along with the contact angle for each coating.

The protection efficiency of the MS10 coating was very high at 99.9 ± 0.1 % (Table 3), and had low contact angle 78 ± 1° (Table 2). The higher protection efficiency of MS10 in comparison to FA5 is most likely related to the chemical bond between the coating and the substrate, which was absent in the FA5 coating as deduced from observing HR spectra for O 1s.

### 3.4.3. *FA5-MS10 coating on sulphide patinated bronze*

For this coating, the changes in C 1s and F 1s spectra in Fig. 9a and b show that the topmost species are F-containing species derived from $CF_2$ and $CF_3$.

Since the MS10 coating provided good protection, the binding of FA and MS, and their binding to $Cu_2S$, are of particular interest.

Below the FA5 layer is the MS10 layer – the latter can be seen in Fig. 9c, where the peak for Si 2p is not pronounced before sputtering, but becomes very intense after the first sputtering cycle of 360 s. As for the MS10 sample, the FA5-MS10 coating most likely bonds to the $Cu_2S$ via O atoms, since the same transition from the position marked by dashed line 2 to the position at dashed line 1 occurs at the end of the sputtering process (from 1080 s to 1440 s sputtering, Fig. 9c). At the end of sputtering (from 1080 s to 1440 s), the signal for the S-containing species (S 2p spectra in Fig. 9e) increases when the excitation signal reaches the $Cu_2S$ present on the substrate. The corresponding depth profile is shown in Fig. 9e.

The protection efficiency of FA5-MS10 coating was 84.4 ± 13 %, while the contact angle was 115.9 ± 0.8°.

### 3.4.4. *FA5-MS10-SH5 coating on sulphide patinated bronze*

For further study by XPS, FA5-MS10-SH5 coating was chosen over FA1-MS10-SH1, which showed higher protection efficiency, due to our previous papers when we used the same blend of the three components. For FA5-MS10-SH5 coating over patinated bronze, it was observed that the topmost position consists of F-containing species originating from $CF_3$ and $CF_2$. The signals representing these species become less intense with sputtering, as can be seen in Fig. 10a and c (the signal for C 1s drops faster than that for F 1s because the XPS relative sensitivity factor for F 1s is much higher than that for C 1s). The topmost position also likely contains oxidized adventitious carbonaceous species (positioned at dashed line 2 in Fig. 10b). The position at dashed line 3 in the O 1s spectra corresponds to the O-containing species in MS10. As in the MS10 and FA5-MS10 samples, the position of the most intense peak in O 1s shifts to a more negative $E_B$ when enough coating has been removed by sputtering for the excitation signal to reach the $Cu_2S$-covered substrate (this occurs after 2925 s, where the signal for S 2p at the position of the dashed line 1 in Fig. 10d, which is from $Cu_2S$, also becomes intense). A less intense, but nevertheless evident signal in the S 2p spectra develops at a more negative $E_B$ (positioned at dashed line 2, spectra after 765–2265 s of sputtering). This signal may correspond to a layer of mercaptopropyltrimethoxy silane (5SH) below the MS10 layer. Disulphide bonds may also potentially be found as a result of inter molecule polymerization. The MS10 layer is below the FA5 layer, as shown by the fact that the spectra of the first sputtering cycles do not show a peak in the Si 2p spectra until 225 s. A peak in the Si 2p spectra developed later (after sputtering for 465–2325 s). The spectra measured before and during sputtering up to 465 s show signals at a more positive $E_B$ compared to the characteristic position of $Cu_2S$ (at dashed lines 3 and 4, Fig. 10d). The latter is most likely the result of partial oxidation of the thiol groups located closer to the uppermost position of the surface.

As shown in Fig. 10f and g, the shape of the XPS-induced Auger Cu LMM and Cu 2p spectra were similar on all the substrate surfaces, including FA5, MS10, FA5-MS10, and FA5-MS10-SH5, in which the sputter beam removes the coating such that the excitation signal reaches the substrate. Fig. 10g shows no shake-up satellites at the position of the dashed lines, indicating that the surface is composed only of Cu(I)-species and/or metallic Cu (i.e. no Cu(II) was present on the surface). On the other hand, the shape of the spectra in Fig. 10f shows that the

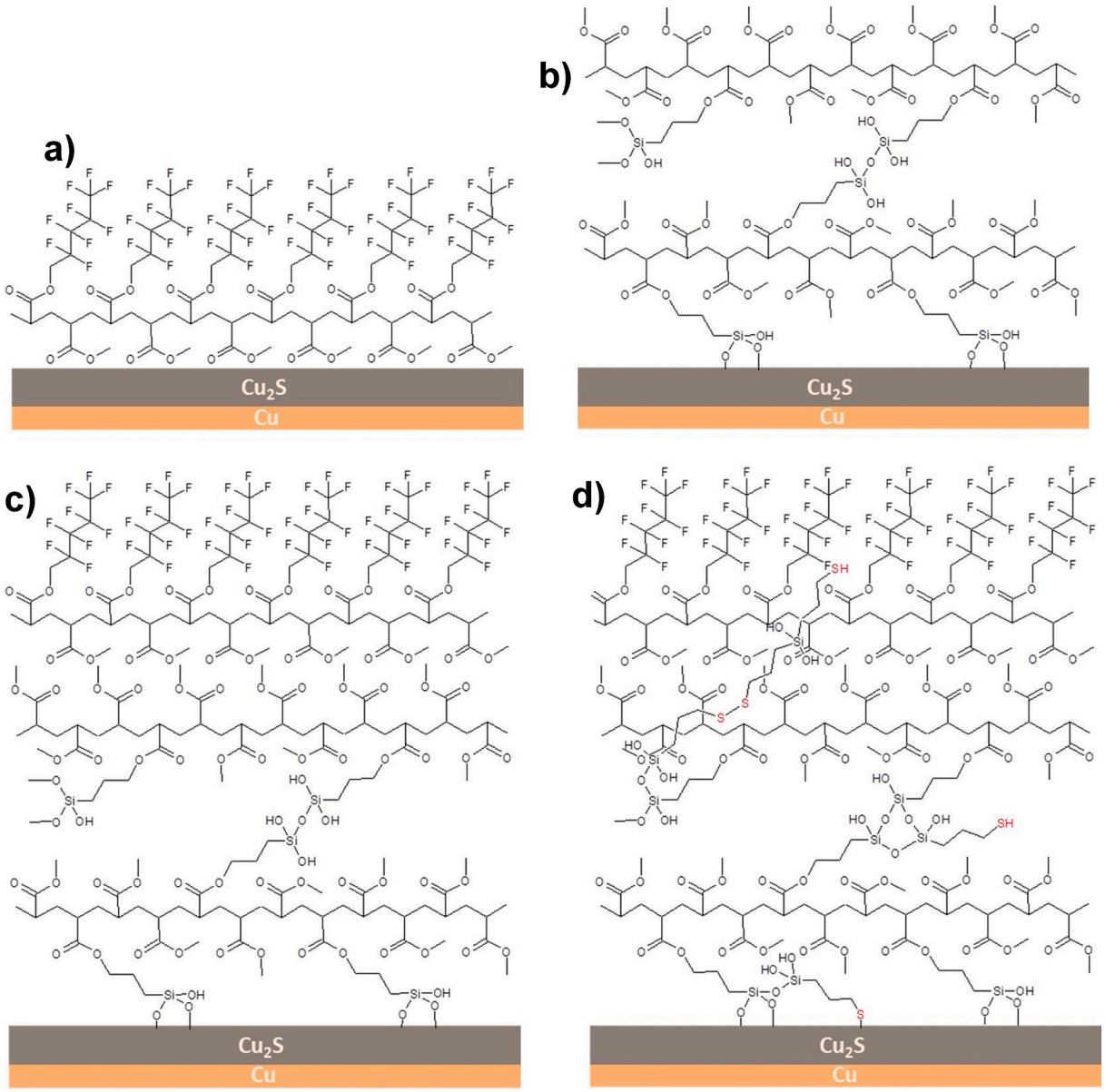


**Fig. 12.** Schematic representation of the potential protection mechanisms of the a) FA5 coating, b) MS10 coating, c) FA5-MS10 coating and d) FA5-MS10-SH5 coating on brown patinated bronze. (For interpretation of the references to colour in this figure, the reader is referred to the web version of this article.)

oxidation state of Cu is Cu(I), with the most intensive feature marked by the dashed line 3 in Fig. 10f. The XPS-induced Cu-LMM spectrum for the Cu species has four characteristic features, as marked by the dashed lines 1–4. The intensity of feature 3 in comparison to the other three features is characteristic for the oxidation state of Cu(I) [32]. Most likely, the surface of the bare substrate (before coating) is primarily composed of $Cu_2S$, with a small amount of $Cu_2O$. The depth profile for the FA5-MS10-SH5 sample is given in Fig. 10h.

The three-component fluoropolymer coating FA5-MS10-SH5 achieved a protection efficiency of 99.4 ± 0.9 %, and the highest contact angle measured was measured on this coating with value 116.4 ± 0.5°. When comparing protection efficiency to MS coating (99.9 %), the three component coating exhibited higher contact angle which is also the preferable property, while MS10 coating had low contact angle measured (Table 2).

### 3.5. AFM analysis

The FA5 coating had a relatively high contact angle due to the hydrophobic nature of the fluoroacrylate coating, although the surface was relatively flat and had few surface irregularities (Fig. 11a). The MS10 coating (Fig. 11b) was very smooth and evenly covered the surface of the patinated bronze. The smooth coverage is likely related to the low contact angle measured for this type of coating (78 ± 1°). The FA5-MS10 coating (Fig. 11c) was relatively rough and had scratches from the grinding process and/or brush marks, resulting in a relatively high contact angle (115.9 ± 0.8°). A similar surface was observed on samples with the FA5-MS10-SH5 coating (Fig. 11d).

### 3.6. Mechanisms of protection

A schematic representation of the fluoroacrylate-FA molecule on the sulphide patina is given in Fig. 12a. The XPS analysis revealed that the fluorocarbon chains are oriented towards the outer surface of the coating, resulting in high hydrophobicity and a contact angle of 114 ± 2°. The oxygen in the ester groups are directed towards the substrate, which consists mainly of cuprous sulphide. Due to the lower protection efficiency (79.8 %), it is suggested that physisorption occurs. However,

lower protection efficiency may be also due to different other factors like patina unevenness.

Once the concentration in the supporting solvent is sufficient, MS offers a high protection efficiency of >99.9 %, while at 78 ± 1° the contact angle in this coating is low. A schematic representation of the orientation of the methacryloxypropyl-trimethoxysilane-MS molecules is presented in Fig. 12b. Silane groups are detected throughout the coating at various sputtering depths, as shown by the XPS analysis presented in Fig. 8. A change in the oxygen signal at the coating-bronze interface indicates that the coating might be adsorbed to the surface via O atoms attached to the Si of the silane groups.

The mechanism of protection of the FA-MS coating is presented in Fig. 12c, with its protection efficiency on the sulphide patina being >84.4 ± 13 %. XPS analysis showed that fluorocarbon chains of the fluoroacrylate (FA) are present at the surface of the coating, as can be observed from the peaks in C1s high resolution spectra (Fig. 9), which also resulted in its high hydrophobicity of 115.9°. The absence of silicon at the surface indicates a good separation between the FA and MS components of the coating. Si is, however, present throughout the entire depth of the coating and the proposed method of bonding to the sulphide patina is, again, via the silanol groups of the MS molecule.

A schematic representation of a possible mechanism of protection for the FA5-MS10-SH5 coating on brown patinated bronze is given in Fig. 12d, in which sulphur atoms from the mercaptosilane are marked in red. XPS analysis showed different peaks for organic sulphur throughout the coating (S 2p in Fig. 10), indicating that mercaptosilane did not preferentially attach to the surface of the brown patina but rather remained evenly distributed throughout the coating. This could explain its low protection against corrosion in comparison to results from the literature [27,28,29].

In addition to the original thiol form of sulphur in the 3-mercaptopropyltrimethoxysilane-SH molecule, oxidized species, such as disulphide and sulphur species containing oxygen of unknown origin, could also be identified.

## 4. Conclusions

Fluoropolymer-based protection systems were tested in order to find the optimal method of protection for the application of sulphide patinated bronze surfaces in outdoor environments. The following conclusions were made:

- A three-component fluoropolymer coating containing fluoroacrylate (FA), silane-modified poly methylmethacrylate (MS) and mercaptopropyltrimethoxy silane (SH) - (FA-MS-SH coating) was studied together with single component applications (FA, MS, SH) and combinations thereof (FA-MS, MS-SH, FA-MS-SH).
- After protecting samples with each of the applied coatings, a darkening occurred in all samples, with the change in colour, i.e. a change in ($\Delta L$).
- Electrochemical testing was conducted to evaluate the protection efficiency. The corrosion study in concentrated simulated rain showed that when brown patinated samples were protected by single components such as SH and FA, the resulting protection efficiency was low. MS protection was also very efficient (>99.9 %), but the contact angle of the coating was low. Using a blend of MS, FA and SH, however, resulted in both, a high protection efficiency of 99.9 % and high hydrophobicity.
- A detailed XPS study made it possible to propose the potential reaction mechanism of the various protective coatings on the sulphide patinated bronze. The protection efficiency varies due to differences in the affinity of the constituent components of the coatings studied. FA5 physisorbed on the surface, while MS10, FA5-MS10 and FA5-MS10-SH5 chemisorbed on the surface. FA5 is arranged with $CF_3$ and $CF_2$ groups on the outer part of the coating containing fluoroacrylate (FA5, FA5-MS10 and FA5-MS10-SH5), resulting in higher hydrophobicity. MS10 attaches to the surface via silanol groups, while in the case of FA5-MS10-SH5 protection, attachment to the surface occurs via silanol and -C-S- groups.

Supplementary data to this article can be found online at https://doi.org/10.1016/j.porgcoat.2022.107071.

## CRediT authorship contribution statement

**Tadeja Kosec:** Conceptualization, Investigation, Writing – original draft, Writing – review & editing, Supervision. **Živa Novak:** Investigation, Formal analysis. **Erika Švara Fabjan:** Validation, Writing – review & editing. **Luka Škrlep:** Investigation, Writing – review & editing. **Matjaž Finšgar:** Investigation, Writing – review & editing.

## Declaration of competing interest

The authors declare that they have no known competing financial interests or personal relationships that could have appeared to influence the work reported in this paper.

## Data availability

Data will be made available on request.

## Acknowledgment

The financial support received from the Slovenian Research Agency (SRA) for programmes P2-0273 and P2-0118 and project NK-0001 is hereby gratefully acknowledged. The project is co-financed by the Republic of Slovenia, the Ministry of Education, Science and Sport, and the European Union through the European Regional Development Fund.

## References

[1] P.A. Schweitzer, Fundamentals of metallic corrosion: atmospheric and media corrosion of metals, in: Corrosion Engineering Handbook, 2nd Ed., CRC Press, Taylor&Francis Group, NY, 2007 https://doi.org/10.1201/9780849382444.
[2] V.N. Naudé, Guide to the Maintenance of Outdoor Sculpture, American Institute for Conservation of Historic and Artistic Works, Washington, D.C., 1993.
[3] F. Ammeloot, C. Fiaud, E.M.M. Sutter, Characterization of the oxide layers on a Cu-13Sn alloy in a NaCl aqueous solution without and with 0.1 M benzotriazole-electrochemical and photoelectrochemical contributions, Electrochim. Acta 44 (1999) (1999) 2549–2558, https://doi.org/10.1016/S0013-4686(98)00391-0.
[4] G. Laguzzi, L. Luvidi, G. Brunoro, Atmospheric corrosion of B6 bronze evaluated by the thin layer activation technique, Corros. Sci. 43 (2001) 747–753, https://doi.org/10.1016/S0010-938X(00)00075-5.
[5] A. Galtayries, A. Mongiatti, P. Marcus, C. Chiavari, Surface characterisation of corrosion inhibitors on bronzes for artistic casting, in Corrosion of Metalic artefacts, P. Dilman Ed, DOPOLNITI.
[6] G. Bierwagen, T.J. Shedlosky, K. Stanek, Developing and testing a new generation of protective coatings for outdoor bronze sculpture, Prog. Org. Coat. 48 (2003) 289–296, https://doi.org/10.1016/j.porgcoat.2003.07.004.
[7] L. Muresan, S. Varvara, E. Stupnišek-Lisac, H. Otmačić, K. Marušić, S. Horvat-Kurbegović, L. Robbiola, K. Rahmouni, H. Takenouti, Protection of bronze covered with patina by innoxious organic, Electrochim. Acta 52 (2007) 7770–7779, https://doi.org/10.1016/j.electacta.2007.02.024.
[8] K. Marušić, H. Otmačić-Ćurković, Š. Horvat-Kurbegović, H. Takenouti, E. Stupnišek-Lisac, Comparative studies of chemical and electrochemical preparation of artificial bronze patinas and their protection by corrosion inhibitor, Electrochim. Acta 54 (2009) 7106–7113, https://doi.org/10.1016/j.electacta.2009.07.014.
[9] K. Rahmouni, H. Takenouti, N. Hajjaji, A. Srhiri, L. Robbiola, Protection of ancient and historic bronzes by triazole derivatives, Electrochim. Acta 54 (2009) 5206–5215, https://doi.org/10.1016/j.electacta.2009.02.027.
[10] T. Kosec, H. Otmačić Ćurković, A. Legat, Investigation of the corrosion protection of chemically and electrochemically formed patinas on recent bronze, Electrochim. Acta 52 (2010) 722–731, https://doi.org/10.1016/j.electacta.2010.09.093.
[11] K. Marušić, H. Otmačić Ćurković, H. Takenouti, Inhibiting effect of 4-methyl-1-p-tolylimidazole to the corrosion of bronze patinated in sulphate medium, Electrochim. Acta 56 (2011) 7491–7502, https://doi.org/10.1016/j.electacta.2011.06.107.
[12] Helena Otmačić Ćurković, Tadeja Kosec, Katarina Marušić, Andraž Legat, An electrochemical impedance study of the corrosion protection of artificially formed

patinas on recent bronze, Electrochimica Acta 83 (2012) 28–39, https://doi.org/10.1016/j.electacta.2012.07.094.
[13] Balbo, C. Chiavari, C. Martini, C. Monticelli, Effectiveness of corrosion inhibitor films for the conservation of bronzes and gilded bronzes, Corros. Sci. 59 (2012) 204–212, https://doi.org/10.1016/j.corsci.2012.03.003.
[14] T. Kosec, A. Legat, P. Ropret, Raman investigation of artificial patinas on recent bronze protected by different azole type inhibitors in an outdoor environment, J. Raman. Spectrosc. 45 (2014) 1085–1092, https://doi.org/10.1002/jrs.4532.
[15] L. Robbiola, et al., New insight into the nature and properties of pale green surfaces of outdoor bronze monuments, Appl. Phys. A Mater. Sci. Process. 92 (2008) 161–169.
[16] C. Chiavari, K. Rahmouni, H. Takenouti, S. Joiret, P. Vermaut, L. Robbiola, Composition and electrochemical properties of natural patinas of outdoor bronze monuments, Electrochim. Acta 52 (2007) 7760–7769, https://doi.org/10.1016/j.electacta.2006.12.053.
[17] P. Ropret, T. Kosec, Raman investigation of artificial patinas on recent bronze - part I: climatic chamber exposure, J. Raman Spectr. 43 (2012) 1578–1586, https://doi.org/10.1002/jrs.4068.
[18] G. Masi, J. Esvan, C. Josse, C. Chiavari, E. Bernardi, C. Martini, M.C. Bignozzi, N. Gartner, T. Kosec, L. Robbiola, Characterization of typical patinas simulating bronze corrosion in outdoor conditions, Mat. Chem. Phys. 200 (2017) 308–321, https://doi.org/10.1016/j.matchemphys.2017.07.091.
[19] G. Masi, C. Josse, J. Esvan, C. Chiavari, E. Bernardi, C. Martini, M.C. Bignozzi, C. Monticelli, F. Zanotto, A. Balbo, E. Svara Fabjan, T. Kosec, L. Robbiola, Evaluation of the protectiveness of an organosilane coating on patinated Cu-Si-Mn bronze for contemporary art, Prog. Org. Coat. 127 (2019) 286–299, https://doi.org/10.1016/j.porgcoat.2018.11.027.
[20] J.-D. Brassard, D.K. Sarkar, J. Perron, Fluorine based superhydrophobic coatings, Appl. Sci. 2 (2012) 453–464, https://doi.org/10.3390/app2020453.
[21] S. Zouari, H. Ghorbel, C. Langlade, H. Liao, R. Elleuch, Painting process design and characterization of polymer coatings on brass, J. Mater. Eng. Perform. 31 (2022) 180–190, https://doi.org/10.1007/s11665-021-06217-x.
[22] K. Startek, S. Arabasz, A. Bachmatiuk, A. Lukowiak, Influence of fluoroalkyl chains on structural, morphological, and optical properties of silica-based coatings on flexible substrate, Opt. Mater. 121 (2021), https://doi.org/10.1016/j.optmat.2021.111524.
[23] I. Milošev, D. Hamulić, P. Rodič, C. Carrière, S. Zanna, H. Budasheva, D. Korte, M. Franko, D. Mercier, A. Seyeux, P. Marcus, Siloxane polyacrylic sol-gel coatings with alkly and perfluoroalkyl chains: synthesis, composition, thermal properties and log-term corrosion protection, Appl. Surf. Sci. 574 (2022), https://doi.org/10.1016/j.apsusc.2021.151578.
[24] N.A. Swartz, C.A. Price, T.Lasseter Clare, Minimizing corrosion of outdoor metalworks using dispersed chemically stabilized nanoclays in polyvinylidene fluoride latex coatings, ACS Omega 1 (1) (2016) 138–147, https://doi.org/10.1021/acsomega.6b00091.
[25] M. Mihelčič, M. Gaberšček, M. Salzano de Luna, M. Lavorgna, C. Giuliani, G. Di Carlo, A.K. Surca, Effect of silsesquioxane addition on the protective performance of fluoropolymer coatings for bronze surfaces, Mater. Des. 178 (2019), 107860, https://doi.org/10.1016/j.matdes.2019.107860.
[26] T. Kosec, L. Škrlep, E. Švara Fabjan, A. Sever Škapin, G. Masi, E. Bernardi, C. Chiavari, C. Josse, J. Esvan, L. Robbiola, Development of multi-component fluoropolymer based coating on simulated outdoor patina on quaternary bronze, Prog. Org. Coat 131 (2019) 27–35, https://doi.org/10.1016/j.porgcoat.2019.01.040.
[27] T. Kosec, Ž. Novak, E.Švara Fabjan, L. Škrlep, A.Sever Škapin, P. Ropret, Corrosion protection of brown and green patinated bronze, Prog. Org. Coat. 161 (2021) 1–9, https://doi.org/10.1016/j.porgcoat.2021.106510.
[28] F. Zucchi, A. Frignani, V. Grassi, G. Trabanelli, M. DalColle, The formation of a protective layer of 3-mercapto-propyl-trimethoxy-silane on copper, Corros. Sci. 49 (2007) 1570–1583, https://doi.org/10.1016/j.corsci.2006.08.019.
[29] C. Chiavari, A. Balbo, E. Bernardi, C. Martini, M.C. Bignozzi, M. Abbottoni, C. Monticelli, Protective silane treatment for patinated bronze exposed to simulated natural environments, Mater. Chem. Phys. 141 (2013) 502–511, https://doi.org/10.1016/j.matchemphys.2013.05.050.
[30] D.A. Shirley, High-resolution X-ray photoemission spectrum of the valence bands of gold, Phys. Rev. B 5 (1972) 4709–4714.
[31] W.S. Mokritzky, M. Tatol, Colour difference Delta E - a survey, Mach. Graph. Vis. 20 (2011) 383–412.
[32] M. Finšgar, X-ray excited auger cu L3L4,5M4,5 spectra measured at low take-off angles as a fingerprint for a cu-organics connection, J. Electron Spectrosc. Relat. Phenom. 222 (Supplement C) (2018) 10–14.